A mathematical model of meat cooking based on polymer-solvent analogy

M. Chapwanya *[1] and N.N. Misra[2]

[1]Department of Mathematics and Applied Mathematics, University of Pretoria, Pretoria 0002, South Africa
[2]School of Food Science & Environmental Health, Dublin Institute of Technology, Dublin 1, Ireland

Abstract

Mathematical modeling of transport phenomena in food processes is vital to understand the process dynamics. In this work, we study the process of double sided cooking of meat by developing a mathematical model for the simultaneous heat and mass transfer. The constitutive equations for the heat and mass transport are based on Fourier conduction, and the Flory-Huggin's theory respectively, formulated for a two-phase transport inside a porous medium. We investigate a reduced one-dimensional case to verify the model, by applying appropriate boundary conditions. The results of the simulation agree well with experimental findings reported in literature. Finally, we comment upon the sensitivity of the model to the porosity of meat.

Keywords: Flory-Huggin's theory; heat and mass transfer; mathematical modeling.

1 Introduction

Since antiquity, thermal processing has remained the technology of choice to improve the eating quality and safety of food products, and to extend their shelf-life. Although within recent years research in food science has largely focused on development of nonthermal technologies [1], thermal processing still remains the most widely used method in the food industries [2]. Of special importance in thermal processing of foods are the meat and meat products. This is because these almost invariably undergo thermal processing at some stage before consumption (with some exceptions). In addition, meat is eaten on a daily basis in many countries. The composition and high moisture content of meat creates an ideal environment for the growth and proliferation of pathogenic and spoilage microorganisms [3]. The major objective of thermal processing and cooking is to guarantee food safety by killing bacteria (for example *Escherichia coli* O157:H7 and *Listeria monocytogenes*) and inactivating their enzymes or other metabolites in foods. The U.S. Department of Agriculture Food Safety and Inspection Service (USDA-FSIS) comparative risk assessment of nonintact and intact beef steaks indicated that oven broiling to an internal temperature

*Corresponding author; E-Mail: m.chapwanya@up.ac.za

of more than 60 °C would result in safe blade-tenderized beef steaks [4, 5]. A common household method for cooking meat (example beef, hamburger or patties) involves simultaneous application of heat from both sides (double sided cooking).

The purpose of a mathematical model of the heat and mass transfer in a food production process is to describe the physical processes as accurately as possible for the given food production process [6]. In order to be able to optimise the cooking of meat, in general, and a beef steak in particular (which is at focus in this study), it is important to develop a well-posed representative mathematical model. In recent past, the importance of mathematical modelling in cooking/roasting process of meat and meat products has been well-emphasised by many researchers [7, 8, 9, 10, 11]. The mathematical models encountered in food science literature often are either empirical or mechanistic (physics-based) [12]. Empirical models are generally obtained from simple mathematical correlation of experimental data, and therefore are data driven. On the other hand, the elementary processes of heat and mass transfer are considered in mechanistic models. The advantage of physics-based mechanistic models is that these provide insight into the physical processes in a manner that is more precise [13].

Many foods, in general, are described as porous matrices by virtue of their structural/cellular arrangement [14, 15]. Meat is composed of bundles of muscle fibers, which are largely protein. The intercellular space within muscle tissues is primarily filled with blood plasma which renders a pressure in the pores when driven by external forces. The plasma can be considered as a newtonian liquid. On the other hand, within the intracellular region the water is bound to the muscle proteins. The water distribution and porous structure of meat can be appreciated from the details provided by van der Sman [16], Dhall et al. [11] and Sun and Hu [17]. Based on the above discussion, it does not come as a surprise that the moisture movement within meat could be dealt with a continuum approach despite the porous structure. Flow in a porous medium is classically described by Darcy's equation for the liquid velocity; nevertheless, appropriate problem-specific couplings and amendments to the equation are also common (for example [18]). The flow under this scenario is driven by a pressure gradient. Extending the porous description of muscle, and drawing analogies from soft condensed matter physics, van der Sman [8, 19] deduced a model for heat and mass transport during cooking of meat. This approach considers that meat is composed of a polymer matrix made of protein and that the Flory-Rehner theory holds true. Under these assumptions, the moisture driving entity when cooking would be the swelling pressure which can be substituted into Darcy's equation. This approach provides far more accurate predictions than the lumped Fickian diffusion considered hitherto [20] and also agrees well with the capillary pressure driven flow description for moisture transport in meat [21]. Inspired by van der Sman's pioneering works, in conjunction with experiments conducted by Shen et al. [22], we focus upon the development of a two-phase, soft condensed matter physics based mechanistic model to simulate the transport phenomena within a beef steak when simultaneously heated from both sides. The presented work differs from [8, 19] in several ways. While van der Sman studied the convective oven cooking of meat using the Flory-Rehner theory, the present work aims at numerically simulating the double sided conductive pan cooking of beef using the simplified Flory-Huggins theory. In addition, we formulate the conservation equations for a two phase mixture (as opposed to the Darcy's porous medium transport alone in [8, 19]) of a polymer and a solvent, both of which are dealt with a continuum approach. Our approach in dealing the protein and solvent phases separately via a two phase model allowed assessing the effect of porosity of meat on cooking time, which has not been studied hitherto. This dynamics of porous structure is of particular importance when heating

smaller pieces of meat, as identified earlier [8]. Furthermore, the model now has sufficient physics to capture the details of the underlying processes, giving better results for thin steaks, even with a one dimensional geometry. We wish to point that the model derived herein has some similarities to, and is based on the polymer-solvent models derived elsewhere in the literature in the context of biofilms; see for example, Winstanley et al. [23] and Cogan and Keener [24].

The structure of the present paper is the following. In the next section, we derive the model based on conservation laws, introduce the polymer-solvent assumption based on Flory-Huggins theory and define the boundary conditions. We then non-dimensionalise, and proceed further by reducing the model to a simpler form. We then study the reduced model in one dimension, and compare with experimental results reported by Shen et al. [22]. Finally, we evaluate the sensitivity of the model to model parameters and discuss the consequences.

2 Model derivation

In Figure 1, a pictorial presentation of the problem in consideration and the geometry is provided for the case where meat is subjected to double sided heating. The lean beef sample (<4% fat) is heated from top and bottom using hot plates maintained at a constant temperature. It is assumed that the surface of meat is completely in contact with the hot plate. Under this scenario, the heat flows from either end towards the centre ($0 < z < L$). As mentioned earlier, the pores are ideally filled with plasma and ions and other soluble proteins. For the present study, we assume that the pores are saturated with water (incompressible fluid) and the solid matrix does not undergo global deformation. We now define ρ_s to be the density of the protein matrix, whose volume fraction is ϕ. Satisfying the criteria of saturation, we have $(1-\phi)$, the volume fraction of the liquid, whose density, we define as ρ_ℓ. Effectively, the model assumes that the pores are completely filled with the liquid phase and therefore, $(1-\phi)$ is also the medium porosity.

In the following sections, we use a multidimensional approach to outline the mathematical model under investigation.

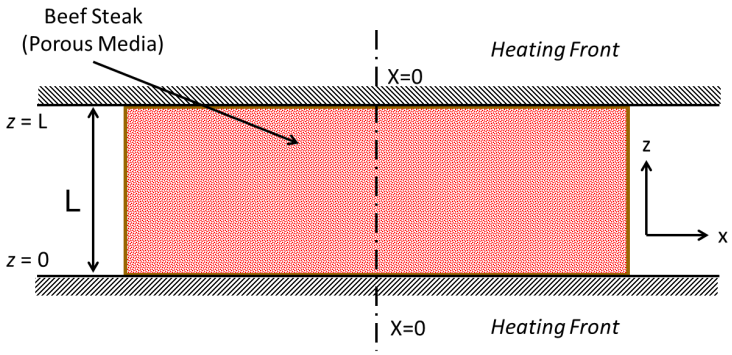

Figure 1: Geometry of the problem for double sided heating

2.1 Conservation of Mass

In the absence of mass exchange, the local law of conservation of mass of the two components governed by the continuity equation reduces to

$$(\phi\rho_s)_t + \nabla.[\phi\rho_s\mathbf{v}] = 0, \tag{2.1}$$
$$([1-\phi]\rho_\ell)_t + \nabla.[(1-\phi)\rho_\ell\mathbf{w}] = 0, \tag{2.2}$$

where **w** is the average fluid velocity, and **v** is an analogous average solid velocity, cf. McGuinness et al. [25]. This essentially accounts for the rate of displacement of the material points of the polymer phase with respect to the corresponding initial coordinates in a Lagrangian frame of reference. The equations also signify that there are no source and sink terms (except at the boundaries); *i.e.* there is no internal heat generation or chemical reactions within the meat matrix. Assuming incompressibility in equations (2.1) and (2.2) we obtain the local mass balance of the system-

$$\phi_t + \nabla.[\phi\mathbf{v}] = 0, \tag{2.3}$$
$$-\phi_t + \nabla.[(1-\phi)\mathbf{w}] = 0. \tag{2.4}$$

2.2 Conservation of Momentum

Considering the assumptions stated earlier, the momentum balance for the system based on Darcy's flow in porous medium reduces to, cf. [23]

$$0 = -f_0\phi(1-\phi)(\mathbf{v}-\mathbf{w}) - \nabla\Psi - \phi\nabla p, \tag{2.5}$$
$$0 = f_0\phi(1-\phi)(\mathbf{v}-\mathbf{w}) - (1-\phi)\nabla p, \tag{2.6}$$

where, f_0 (Pa s m^{-2}) is the microscale interfacial friction term, p is the fluid pressure and Ψ is the osmotic pressure, gradients of which create the force on the polymer (meat proteins). This term has also been referred to as the 'inter-phase pressure' in two-phase fluid models [26]. The equations take into account the fact that the protein matrix acts like a sponge, which loses a significant amount of liquid water when receiving some stimuli (e.g. stress-strain due to protein denaturation) [10, 27]. Moving further, summation of equation (2.5) and equation (2.6) yields the local momentum balance of the system

$$\nabla\Psi = -\nabla p. \tag{2.7}$$

Based on Flory Rehner theory, van der Sman [16] has shown that the swelling pressure (so termed after the swelling of polymers) can be replaced into the Darcy's equation as the driving pressure. In the context of cooking of meat, this pressure gradient arises from the water potential difference due to the deformation of meat proteins, as they undergo denaturation. Following the same school of thought, we introduce the osmotic pressure Ψ, which is a direct outcome of the Flory-Huggins theory, expressed as

$$\Psi = -E\left[\ln(1-\phi) + \left(1-\frac{1}{n}\right)\phi + \chi(T,\phi)\phi^2\right], \tag{2.8}$$

where $E = RT_0/V > 0$ is the lattice energy density, $\chi(T,\phi)$ is the temperature and moisture dependent Flory-Huggins interaction parameter, n is the ratio of molar volumes of solute (protein) and solvent (water), R [J mol^{-1} K^{-1}] is the gas constant, T_0 [K] is the temperature and V

[$\mathrm{m}^3\,\mathrm{mol}^{-1}$] is the molar volume of water. The underpinning principles of the theory are based on balancing the chemical potentials of the system. Proceeding further, if n is sufficiently large ($n \to \infty$), which is a valid assumption for the case of lean beef (rich in protein- a biopolymer), equation (2.8) can be simplified to

$$\Psi = -E\left[\ln(1-\phi) + \phi + \chi(T,\phi)\phi^2\right]. \tag{2.9}$$

Following [16], we take $\chi(T,\phi)$ in the form

$$\chi(T,\phi) = \chi_p(T) - (\chi_p(T) - \chi_0)(1-\phi)^2, \tag{2.10}$$

where $\chi_0 = 0.5$ is the interaction parameter for fully hydrated polymer (meaning that the polymer/proteins are distributed in a way such that they are in maximum contact with water) and $\chi_p(T)$ is the temperature dependent interaction parameter.

The physical significance for the temperature dependency arises from the fact that proteins undergo denaturation to various degrees depending on the temperature. The term $\chi_p(T)$ is given by a Logistic type of sigmoidal function

$$\chi_p(T) = \chi_{pn} - \frac{\chi_{pd} - \chi_{pn}}{1 + A\exp(-\gamma[T - T_e])}, \tag{2.11}$$

where, χ_{pn} is the interaction parameter of dry, *native* meat protein, χ_{pd} is the interaction parameter for the denatured protein, γ (K^{-1}), $T_e(K)$, and A are parameters of the equation obtained by nonlinear least squares fitting to the data for WHC versus temperature (K). In Figure 2 we show the functional relationships (2.10) and (2.11) for the temperature range under investigation.

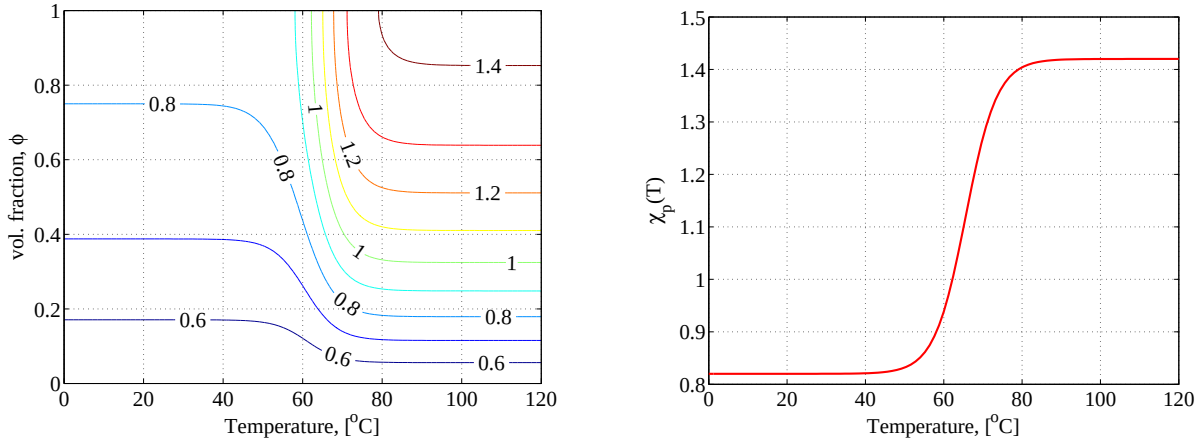

(a) (b)

Figure 2: The relation between the variables in equation (2.10) – (a), and equation (2.11) – (b), for the parameter values in Table 1.

2.3 Conservation of Energy

Heat is transported within the meat primarily by conduction with the latent heat related to chemical changes within the meat being negligible. Accordingly, the energy balance equation for the system

Symbol	Definition	Value	Units	Source
$1-\phi_0$	Initial porosity	0.0128		[28]
T_o	Initial meat temperature	277.15	K	
k_ℓ	Liquid thermal conductivity	0.57	W/mK	[29]
k_s	Matrix thermal conductivity	0.18	W/mK	[29]
L	Meat thickness	0.025	m	[22]
c_s	Matrix heat capacity	2008	J/kgK	[29]
c_ℓ	Heat capacity of water	4178	J/kgK	[29]
ρ_s	Matrix density	1330	kg/m^3	[29]
ρ_ℓ	Density of water	997.2	kg/m^3	[29]
E	Lattice energy density	1.25×10^8	N/m^2	
f_0	Interfacial friction term	6.26×10^{15}	Pa s m^{-2}	
$\Delta T+T_0$	Temperature of hot plate	449	K	[22]
χ_{pn}	Sigmoid curve Parameter	0.74		[8]
$\chi_{pd}-\chi_{pn}$	Sigmoid curve Parameter	0.345		[8]
A	Sigmoid curve Parameter	30		[8]
γ	Sigmoid curve Parameter	0.25		[8]
T_e	Centre of sigmoidal fit	325 K		[8]

Table 1: Typical values of the parameters used in the model.

is given by a nonlinear form of the Fourier's second law in the porous medium

$$(cT)_t+\nabla.[\rho_\ell c_\ell \mathbf{w}(1-\phi)T]=\nabla.(k\nabla T), \tag{2.12}$$

where c and k are the weighted specific heat capacity and thermal conductivity respectively (c.f. [30, p. 233]) given by,

$$c=\phi\rho_s c_s+(1-\phi)\rho_\ell c_\ell, \tag{2.13}$$
$$k=\phi k_s+(1-\phi)k_\ell. \tag{2.14}$$

The subscripts ℓ and s denote the liquid (solvent) and the solid (polymer) protein matrix respectively. It is well-recognised that the thermal conductivity and heat capacity of meat change with temperature. This is taken into account via equations (2.13) and (2.14) as c and k_m are dependent on ϕ, which itself is a function of temperature and space. Using equations (2.1), (2.2) and (2.13), the energy equation (2.12) may be reduced to

$$cT_t+\rho_s c_s T\phi_t+\rho_\ell c_\ell(1-\phi)\mathbf{w}.\nabla T=\nabla.(k\nabla T). \tag{2.15}$$

2.4 Boundary and initial conditions

To close the system, we have to specify the boundary and initial conditions. In the case of double sided heating, a certain temperature is kept constant during processing. Initially, the meat is assumed to have porosity $1-\phi_0$ at a temperature $T=T_0$. At the boundary in contact with the hot

plates (at $z = 0$ and $z = L$) we have

$$T = T_0 + \Delta T, \tag{2.16}$$

$$\mathbf{w} = 0, \tag{2.17}$$

$$\frac{\partial \phi}{\partial n} = \frac{\partial \Psi}{\partial n} = 0, \tag{2.18}$$

where ΔT is the prescribed temperature drop.

2.5 Parameter estimation

The values of parameters used in this work are summarised in Table 1. As highlighted in [14, 31], many of the parameter values required for mathematical modelling of food processes are nonexistent in the food science literature. Therefore, for the present model the value of the interfacial friction term, f_0 is estimated from $f_0 \sim \dfrac{\mu(1-\phi_0)}{K\phi_0}$, cf. [23], where μ is the viscosity of water and K is the permeability. With $\mu \sim 998$ [Pa s] and $K \sim 2.047 \times 10^{-15}$ [m^2] [11, 14], we have $f_0 \sim 6.26 \times 10^{15}$ [Pa s m^{-2}]. The value of the lattice energy density depends on the temperature and ranges between 1.25×10^8 to 1.58×10^8 [N/m^2] for 273.15 K and 343.15 K respectively. Here, for simplification, we assume it is constant and estimate at $T_0 = 273.15$ K.

3 Non-dimensionalisation

We choose the following explicit scales for non-dimensionalisation by suitable balance of equations. Specifically, we balance

$$t \sim t_0 = \frac{c_\ell \rho_\ell d^2}{k_\ell} = \frac{d^2}{\kappa_\ell}, \quad \Psi, p \sim p_0 = f_0 \kappa_\ell, \quad \mathbf{v}, \mathbf{w} \sim v_0 = \frac{\kappa_\ell}{d}, \quad \mathbf{x} \sim d, \quad T - T_o \sim \Delta T,$$

where $\kappa_\ell = k_\ell/(c_\ell \rho_\ell)$ is the thermal diffusivity of the liquid. We now have the following scaled equations

$$\phi_t + \nabla.[\phi \mathbf{v}] = 0, \tag{3.1}$$

$$-\phi_t + \nabla.[(1-\phi)\mathbf{w}] = 0, \tag{3.2}$$

$$0 = -\phi(1-\phi)(\mathbf{v} - \mathbf{w}) - \nabla\Psi - \phi\nabla p, \tag{3.3}$$

$$0 = \phi(1-\phi)(\mathbf{v} - \mathbf{w}) - (1-\phi)\nabla p, \tag{3.4}$$

$$cT_t + (\alpha + \nu T)\phi_t = -(1-\phi)\mathbf{w}.\nabla + \nabla.(k\nabla T), \tag{3.5}$$

$$\Psi = -\beta \left[\ln(1-\phi) + \phi + \chi(T,\phi)\phi^2\right], \tag{3.6}$$

where

$$c = 1 - \phi(1-\nu), \quad k = 1 - \phi(1-\omega),$$

and

$$\chi(T,\phi) = \chi_p(T) - (\chi_p(T) - \chi_0)(1-\phi)^2, \quad \chi_p(T) = \chi_{pn} - \frac{\chi_{pd} - \chi_{pn}}{1 + \theta \exp(-\Gamma T)},$$

with $\theta = A\exp(-\gamma[T_0 - T_e]) = 4.7 \times 10^6$, and $\Gamma = \gamma\Delta T = 44.0$. The nondimensional form of the equations accommodates various products as well as cooking parameters. The dimensionless parameters are defined as follows

$$\nu = \frac{\rho_s c_s}{\rho_\ell c_\ell}, \quad \omega = \frac{k_s}{k_\ell}, \quad \beta = \frac{E}{f_0 \kappa_\ell}, \quad \alpha = \frac{\nu T_o}{\Delta T},$$

and their typical values are given in Table 2. In these equations ν is the effective volumetric heat capacity, ω is the effective conductivity and β measures the ability of the moisture to flow through the matrix. The advantage of the proposed dimensional analysis is that the two estimated parameters are now defined by a single parameter β whose significance will be investigated further under the numerical section.

Parameter	Value
ν	0.8218
ω	0.3158
β	0.1140
α	1.295

Table 2: Typical values of the dimensionless parameters.

Equations (3.1) and (3.3) can be combined to give

$$\nabla.[\phi(\mathbf{v} - \mathbf{w})] + \nabla.\mathbf{w} = 0. \tag{3.7}$$

On the other hand, substituting (2.7) into (3.6) we have

$$\phi(\mathbf{v} - \mathbf{w}) = -\nabla\Psi,$$

or

$$\mathbf{v} = \mathbf{w} - \frac{1}{\phi}\nabla\Psi. \tag{3.8}$$

Combining (3.7) and (3.8) we have

$$\nabla.\left[\mathbf{w} - \nabla\Psi\right] = 0. \tag{3.9}$$

We now have a system of four equations in four unknowns, namely $\phi,\ T,\ \mathbf{w},\ \Psi$, i.e.,

$$\begin{aligned}
\phi_t &= \nabla.[(1-\phi)\mathbf{w}], \\
cT_t + (\alpha + \nu T)\phi_t &= -(1-\phi)\mathbf{w}.\nabla T + \nabla.(k\nabla T), \\
0 &= \nabla.\left[\mathbf{w} - \nabla\Psi\right], \\
\Psi &= -\beta\left[\ln(1-\phi) + \phi + \chi(T,\phi)\phi^2\right].
\end{aligned}$$

We highlight that all the parameters, except β, are $\mathcal{O}(1)$. The model will be solved numerically.

It is worth mentioning that in the limit $\beta = 0$, the model reduces to a heat conduction problem. This is because β relates the moisture transport to that of the heat transport. While such models do exist in the literature (see for example [7, 9]), they have limitations in that they completely ignore the transport of moisture.

3.1 Reduced Model

Aligning with our previously stated objective of development of a mechanistic model based on Flory-Huggins theory, we now focus upon reducing the model to a one-dimensional case. For the sake of simplicity, we assume the meat block to extend to infinite length, such that any boundary effects are ruled out. For a one dimensional model taken along direction z, we summarise the equations as follows

$$\begin{aligned} \phi_t &= [(1-\phi)w]_z, \\ cT_t + (\alpha + \nu T)\phi_t &= -(1-\phi)wT_z + (kT_z)_z, \\ w &= \Psi_z, \\ \Psi &= -\beta\left[\ln(1-\phi) + \phi + \chi(T,\phi)\phi^2\right]. \end{aligned}$$

Or simply

$$\phi_t = [(1-\phi)\Psi_z]_z, \tag{3.10}$$

$$cT_t + (\alpha + \nu T)\phi_t = -(1-\phi)\Psi_z T_z + (kT_z)_z, \tag{3.11}$$

where

$$c = 1 - \phi(1-\nu), \quad k = 1 - \phi(1-\omega),$$

and $\Psi = \Psi(T, \phi)$. This one dimensional reduction is based the assumption that there is no normal flow at the heated surface ($z = 0$), and $\partial\Psi/\partial n = w = 0$. We see that the volume fraction of the protein satisfies a nonlinear diffusion equation and from a mathematical point of view, one can check the well-posedness of this equation. As originally proposed by Flory [32, 33], we may assume that χ is independent of the composition (ϕ) and temperature (T) so that

$$\begin{aligned} \phi_t &= (\Lambda\phi_z)_z, \\ cT_t + (\alpha + \nu T)\phi_t &= -\Lambda\phi_z T_z + (kT_z)_z. \end{aligned}$$

where $\Lambda = (1-\phi)\dfrac{d\Psi}{d\phi}$, which, under this assumption, can be simplified to

$$\Lambda = 2\beta\phi\left[\left(\tfrac{1}{2} - \chi\right) + \chi\phi\right].$$

Hence we require that $\phi > \dfrac{\chi - \frac{1}{2}}{\chi}$ with $\chi > \frac{1}{2}$. At this point a comment on the Flory's interaction parameter, χ is appropriate. The critical value of χ for miscibility of a polymer in a solvent is approximately 0.5. For values of χ less than 0.5 the polymer will be soluble in the solvent, hence the choice $\chi_0 = 0.5$ in equation (2.10). However, the analogous polymer-solvent theory for meat requires that the polymeric proteins be insoluble in the solvent, water. Therefore, our assumption of $\chi > \frac{1}{2}$ is physically valid, for only with this constraint the polymer will not be soluble in the solvent [32].

3.2 Numerical Simulations

Our numerical strategy for solving the equations for ϕ and T involves the use of a finite difference scheme by dividing the problem domain into N equidistant nodes. We have $\Delta z = 1/N$, the cell width with cell centres $z_i = (i - \frac{1}{2})\Delta z$ for $i = 1, 2, 3, \cdots, N$. Using this notation, we discretise the set of partial differential equations using the method of lines as follows.

$$(\phi_i)_t = \frac{1}{\Delta z}\left[\Theta_{i+1/2}\frac{\phi_{i+1}-\phi_i}{\Delta z} - \Theta_{i-1/2}\frac{\phi_i - \phi_{i-1}}{\Delta z}\right] + \frac{1}{\Delta z}\left[\Omega_{i+1/2}\frac{T_{i+1}-T_i}{\Delta z} - \Omega_{i-1/2}\frac{T_i - T_{i-1}}{\Delta z}\right] \tag{3.12}$$

$$c_i\,(T_i)_t + [\alpha + \nu T_i]\,(\phi_i)_t = -\left[\Theta_i\frac{\phi_{i+1/2}-\phi_{i-1/2}}{\Delta z} + \Omega_i\frac{T_{i+1/2}-T_{i-1/2}}{\Delta z}\right]\frac{T_{i+1/2}-T_{i-1/2}}{\Delta z} + \frac{1}{\Delta z}\left[k_{i+1/2}\frac{T_{i+1}-T_i}{\Delta z} - k_{i-1/2}\frac{T_i - T_{i-1}}{\Delta z}\right] \tag{3.13}$$

for equations (3.10) and (3.11) respectively. Here we have defined

$$\Theta = (1-\phi)\frac{\partial \Psi}{\partial \phi},$$

and

$$\Omega = (1-\phi)\frac{\partial \Psi}{\partial T}.$$

The system of nonlinear ODEs are then integrated with Matlab's standard stiff solver ODE15s, whose resolution algorithm is based on the numerical differentiation formula method (improved version of the implicit Backward Differentiation Formula method). The solution code written in MATLAB (The MathWorks, MA, USA) was run on a 3.0 GHz Intel Core i7 processor. For all the simulations presented in this paper, we use $N = 201$ and we found no visible change in results to the naked eye upon rerunning the simulations with increased number of nodes.

4 Results and Discussion

In this section we present computational results for the different steaks (1.5 cm, 2.5 cm and 4.0 cm thick steak) and we end by presenting a sensitivity analysis for both the choice of initial porosity and parameter β. In each case, the computations are stopped once the centre temperature of the steak reaches 65 ^{o}C to give the simulated cooking time. The model performance will be based on the comparison between cooking time obtained from the model and the experiments.

4.1 Temperature and Moisture Evolution

Figure 3 (a) shows the simulated temperature profile in the beefsteak during double sided heating at equally spaced time intervals. The parameters were chosen based on the 1.5 cm steak, see [22]. We observe that as the heat flows by conduction described by the Fourier equation in our model, the interior temperature rises slowly at both heating ends. Also, we note that the temperature equilibrates in the interior of the meat as time proceeds. It may be noted that this typical profile

of the heat transfer will be obtained irrespective of a 1-D or 2-D approach, given the temperature profile is evaluated at the central axis of the steak [7]. However, when considering the spatial temperature profile, the edges of the meat sample are open to the ambient environment which causes a heat loss. This distinct temperature profile at edges can easily be captured with a 2-D approach by employing a convective cooling boundary condition. Finally, we also observe from figure 3 (a) that the temperature at the core/geometric centre of the meat of thickness 1.5 cm reaches a temperature of 65 °C in 4.24 min. This is in agreement with the experimental results reported by Shen et al. [22].

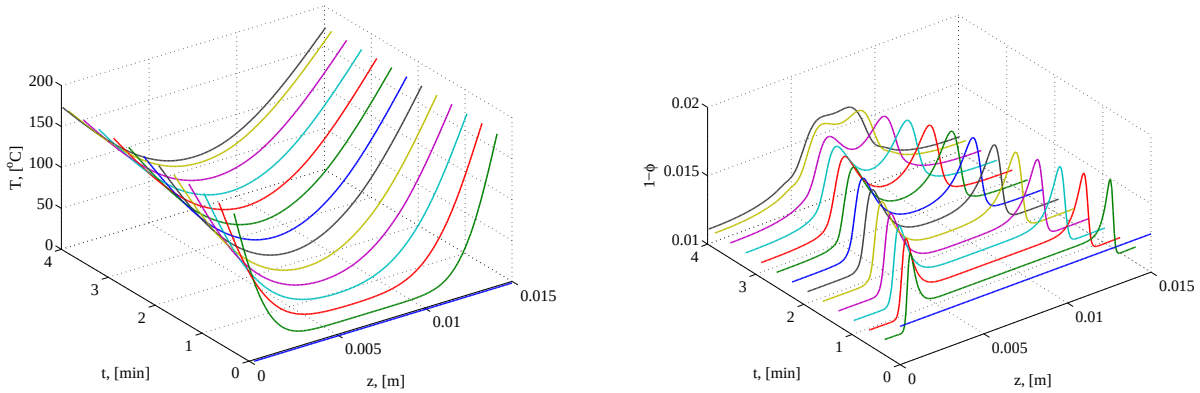

(a) Temperature profiles. (b) Moisture profiles.

Figure 3: Simulated (a) temperature and (b) moisture profiles inside a 1.5 cm thick beefsteak obtained using the 1-D model for double sided heating.

Figure 3 (b) shows the moisture profile inside the beefsteak under simulated conditions. We note that the evolution of the moisture profile closely resembles travelling waves approaching towards each other. We also observe that the moisture is driven towards the centre, as a consequence of which, a rise in the local moisture content in the central region of the steak follows. This phenomenon was reported during previous simulations [8], and was also observed experimentally [34, 35]. The observed effect is due to the internal changes in the volume fraction of the two phases driven by the changing osmotic pressure. While we recognise that the mechanism of water diffusion within a porous solid is complex [36], we attempt to explain the aforementioned observation as the following. Around 80% of the water in the muscle is held within the myofibrils in the spaces between the thick and the thin filaments and this water redistributes only following changes in this spacing [27]. Upon heating, the muscle fibres (connective tissue) undergo shrinkage which exerts a positive pressure and expels the water towards the extracellular porous zone. We wish to point to the fact that the shrinkage and swelling of myofibrils is a crucial factor in raw beef, whereas the ability of meat proteins to form different types of gel dominates in comminuted meat products (e.g. beef patties) [27].

Recently, Tom et al. [37] employed Kelvin equation and Halsey equation to determine the average pore size of beef. The authors report that the pores enlarge with increase in moisture levels and sorption temperature. It should be noted that the porosity in [37] refers to volume fraction of solvent $(1 - \phi)$ in our case. We now observe from Figure 3 (b) that the porosity and moisture follow this relation and also support the observations made by Tom et al. [37].

4.2 Model Validation

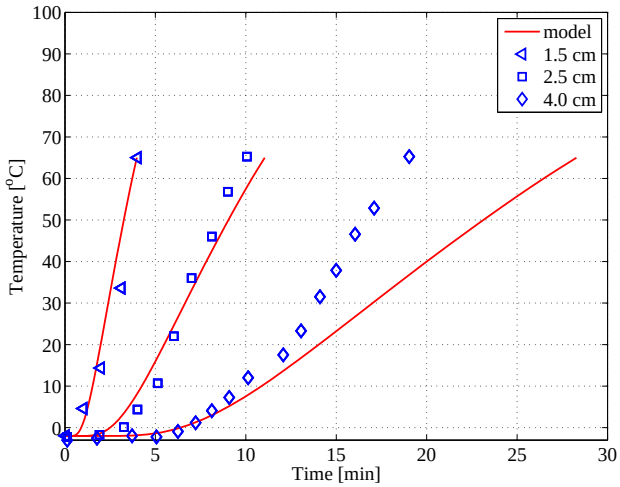

Figure 4: Evolution of the experimental [22] (open symbols) and simulated temperatures (solid line) at the geometric centre.

In order to validate the model, we set-up the parameters for numerical simulations as per those reported in Shen et al. [22] and use material property values mentioned in Table 1, unless otherwise explicitly stated. Figure 4 (a) presents the evolution of both experimental [22] and simulated beefsteak temperature profiles for double sided cooking. Firstly, we observe that the temperature of the geometric centre of the steak shows a continuous increase. Secondly, the time to reach a core temperature for satisfying the microbial safety criteria increases with increase in thickness of the beef steak. For evaluating the accuracy of the models, we employ the statistical criterion of the Root Mean Squared Error (RMSE).

We find the RMSE for the 1.5 cm, 2.5 cm and 4.0 cm thick steak to be 4.8 ^{o}C, 4.4 ^{o}C and 11.5 ^{o}C respectively. We note that when the sample becomes very thick, the discrepancy in model prediction for core temperature compared to the experimental data significantly increases. We suspect this to be a combined outcome of an increased anisotropy in material properties due to inclusion of fat, and crust formation during cooking of meat in the experimental conditions, which admittedly is not captured by the present model. Further work is needed to improve predictions for thick steaks. Thus, we conclude that the results of our 1-D simulation are in good agreement with the experimentally observed values for steaks of small thickness.

4.3 Sensitivity analysis

We wish to highlight the difficulty that we encountered in selection of appropriate initial porosity value for beef from those reported in literature (see Table 3). The said issue stems from the different estimation methods, together with the variation in food composition and physical structure [12]. In order to address this issue, we performed sensitivity analysis to evaluate the effect of initial porosity on the model estimates.

During heating of meat (or porous foods in general), dynamics of the porous structure becomes important for the analysis of transport processes. The time taken for the geometric centre tempera-

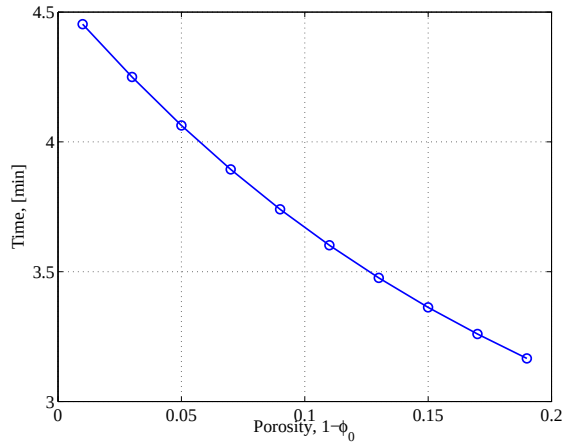

(a) Sensitivity to porosity.

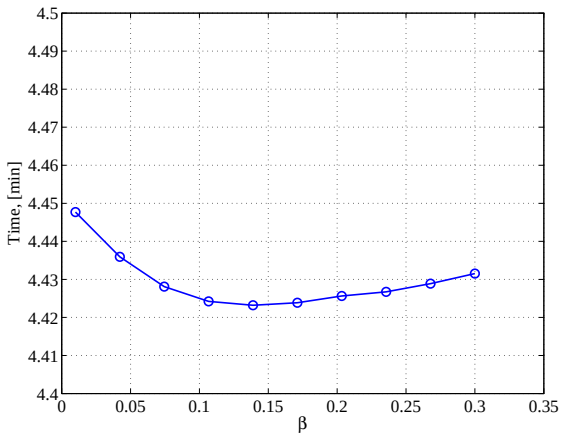

(b) Sensitivity to β.

Figure 5: Time for centre temperature to reach 65 ^{o}C for a 1.5 cm thick beefsteak as a function of (a) porosity and (b) β.

Description	Value	Reference
Raw Beef	0.0128	[28]
Beef	0 – 0.5	[38]
Beef	0.05	[39]
Beef	0.023 – 0.075	[40]
Cooked Beef	0.02313	[41]
Cooked Beef	0.023 – 0.075	[40]

Table 3: Porosity of Beef

ture of a 1.5 cm thick steak to reach 65 ^{o}C as a function of the volume fraction of protein is typified in Figure 5(a). We note a quadratically decreasing trend between the two entities. Conversely, with an increase in porosity by 10%, an decrease in the cooking time by up to 0.8 min can be noticed. This is also partly explained by the fact that the thermal conductivity of the liquid phase is greater than that of the polymeric protein matrix (see Table 1).

Since there is some uncertainty in the choice of interfacial friction term, f_0, which is also related to the parameter β, it is helpful to consider the effects of changes in β on the cooking time. Results are presented in Figure 5 (b), where we fixed the porosity and varied β in the range 0.01 to 0.3. The results indicated deviations of up to 6 seconds in cooking time for the considered values of β. We also notice that the cooking time increases as $\beta \to 0$.

5 Conclusion

The proposed model describes a simultaneous heat and mass transfer model to simulate the double-sided pan cooking of meat. The heat transfer within the matrix of the meat is described using Fourier's law and the moisture transfer is described using the polymer-solvent description given by Flory-Huggin's theory. The principal novelty of the model is that it combines a two-phase

fluid flow and functional equations based on Flory-Huggin's theory that contains microscopically measurable parameters. The model demonstrated good predictive capabilities for core temperature of the beefsteak. The model has some issues in predicting temperatures for thicker steaks that needs to be addressed. Sensitivity analysis indicated that a appropriate selection of initial porosity of meat is vital to obtaining accurate predictions.

Although we considered the case of double sided heating to demonstrate the validity of the model, the modification of boundary conditions for other cases of single sided heating with flipping, oven roasting or frying should be straightforward. The shrinkage during cooking of the steak can be easily incorporated using an appropriate functional relationship of the experimentally determined steak width/radii change with time. A similar approach has been used for modeling the hydration phenomenon in rice by Bakalis et al. [42]. Furthermore, with incorporation of equations for microbial inactivation, this model could also be used to predict microbial safety.

Acknowledgements

MC acknowledges the support of South African DST/NRF SARChI Chair on Mathematical Models and Methods in Bioengineering and Biosciences (M^3B^2). Thanks are also addressed to the three anonymous reviewers whose suggestions have contributed to the improvement of the paper.

References

[1] N. N. Misra, S. U. Kadam, and S. K. Pankaj. An overview of nonthermal technologies in food processing. *Indian Food Industry*, 30:45–52, 2011.

[2] R. S. Kaluri and T. Basak. Role of distributed heating on enhancement of thermal mixing for liquid food processing with heat flow visualization method. *Innovative Food Science & Emerging Technologies*, 18:155–168, 2013.

[3] G. H. Zhou, X. L. Xu, and Y. Liu. Preservation technologies for fresh meat- A review. *Meat Science*, 86:119–128, 2010.

[4] USDA-FSIS. Comparative risk assessment for intact (non-tenderized) and non-intact (tenderized) beef: executive summary. *U.S. Department of Agriculture Food Safety and Inspection Service*, 2002. URL http://www.fsis.usda.gov/PDF/Beef_Risk_Assess_ExecSumm_Mar2002.pdf.

[5] C. Shen, I. Geornaras, K. E. Belk, G. C. Smith, and J. N. Sofos. Inactivation of *Escherichia coli* O157:H7 in moisture-enhanced nonintact beef by pan-broiling or roasting with various cooking appliances set at different temperatures. *Journal of Food Science*, 76:64–71, 2011.

[6] A. H. Feyissa, K. V. Gernaey, and J. Adler-Nissen. Uncertainty and sensitivity analysis: Mathematical model of coupled heat and mass transfer for a contact baking process. *Journal of Food Engineering*, 109:281–290, 2012.

[7] S. E. Zorrilla and R. P. Singh. Heat transfer in double-sided cooking of meat patties considering two-dimensional geometry and radial shrinkage. *Journal of Food Engineering*, 57:57–65, 2003.

[8] R. G. M. van der Sman. Moisture transport during cooking of meat: An analysis based on Flory-Rehner theory. *Meat Science*, 76:730–738, 2007.

[9] D. Ou and G. S. Mittal. Single-sided pan frying of frozen hamburgers with flippings for microbial safety using modeling and simulation. *Journal of Food Engineering*, 80:33–45, 2007.

[10] Sandro M. Goñi and Viviana O. Salvadori. Prediction of cooking times and weight losses during meat roasting. *Journal of Food Engineering*, 100:1–11, 2010.

[11] A. Dhall, A. Halder, and A. K. Datta. Multiphase and multicomponent transport with phase change during meat cooking. *Journal of Food Engineering*, 113:299–309, 2012.

[12] M. Ghafoor, N. N. Misra, K. Mahadevan, and B. K. Tiwari. Ultrasound assisted hydration of navy beans (*Phaseolus vulgaris*). *Ultrasonics Sonochemistry*, 21:409–414, 2013.

[13] S. S. Sablani and A. K. Datta. Mathematical modeling techniques in food and bioprocesses. In M. Shafiur Rehman Shyam S. Sablani, Ashim K. Datta and Arun S. Mujumdar, editors, *Handbook of Food and Bioprocess Modeling Techniques*, chapter 1. CRC Press, 2006. ISBN 978-0-8247-2671-3.

[14] A. K. Datta. Porous media approaches to studying simultaneous heat and mass transfer in food processes. II: Property data and representative results. *Journal of Food Engineering*, 80: 96–110, 2007.

[15] A. K. Datta. Porous media approaches to studying simultaneous heat and mass transfer in food processes. I: Problem formulations. *Journal of Food Engineering*, 80:80–95, 2007.

[16] R. G. M. van der Sman. Modeling cooking of chicken meat in industrial tunnel ovens with the Flory-Rehner theory. *Meat Science*, in-press, 2013.

[17] D-W. Sun and Z. Hu. CFD predicting the effects of various parameters on core temperature and weight loss profiles of cooked meat during vacuum cooling. *Computers and Electronics in Agriculture*, 34:111–127, 2002.

[18] M. Chapwanya and J. M. Stockie. Numerical simulations of gravity-driven fingering in unsaturated porous media using a nonequilibrium model. *Water Resources Research*, 46:W09534, 2010.

[19] R. G. M. van der Sman. Soft condensed matter perspective on moisture transport in cooking meat. *AIChE Journal*, 53:2986–2995, 2007.

[20] G. K. Vagenas, D. Marinos-Kouris, and G. D. Saravacos. An analysis of mass transfer in air-drying of foods. *Drying Technology*, 8:323–342, 1990.

[21] A. K. Datta, R. van der Sman, T. Gulati, and A. Warning. Soft matter approaches as enablers for food macroscale simulation. *Faraday Discussions*, 158:435, 2012.

[22] C. Shen, J. M. Adler, I. Geornaras, K. E. Belk, G. C. Smith, and J. N. Sofos. Inactivation of Escherichia coli O157:H7 in nonintact beefsteaks of different thicknesses cooked by pan broiling, double pan broiling, or roasting by using five types of cooking appliances. *Journal of Food Protection*, 73:461–469, 2010.

[23] H. F. Winstanley, M. Chapwanya, M. J. McGuinness, and A. C. Fowler. A polymer-solvent model of biofilm growth. *Proceedings of the Royal Society A: Mathematical, Physical and Engineering Science*, 467:1449–1467, 2011.

[24] N. G. Cogan and J. P. Keener. The role of the biofilm matrix in structural development. *Mathematical Medicine and Biology*, 21(2):147–166, 2004.

[25] M. J. McGuinness, C. P. Please, N. Fowkes, P. McGowan, L. Ryder, and D. Forte. Modelling the wetting and cooking of a single cereal grain. *IMA Journal of Management Mathematics*, 11:49–70, 2000.

[26] D. A. Drew. Mathematical modeling of two-phase flow. *Annual Review of Fluid Mechanics*, 15:261–291, 1983.

[27] E. Tornberg. Effects of heat on meat proteins- implications on structure and quality of meat products. *Meat Science*, 70:493 – 508, 2005.

[28] K. McDonald and D-W. Sun. The formation of pores and their effects in a cooked beef product on the efficiency of vacuum cooling. *Journal of Food Engineering*, 47:175 – 183, 2001.

[29] Y. Choi and M. R. Okos. *Thermal properties of liquid foods - review*, pages 35–77. American Society of Agricultural Engineers, 1986.

[30] A. C. Fowler. *Mathematical models in the applied sciences*. Cambridge University Press, 1997.

[31] M. Chapwanya and N. N. Misra. A soft condensed matter approach towards mathematical modelling of mass transport and swelling in food grains. *Journal of Food Engineering*, 145: 37–44, 2015.

[32] P. J. Flory. Thermodynamics of high polymer solutions. *Journal of Chemical Physics*, 10:51, 1942.

[33] R. P. Danner and M. S. High. *Fundamentals of polymer solution thermodynamics*, chapter 2, pages 8–9. American Institute of Chemical Engineers, 1993. ISBN 0816905797.

[34] K. Thorvaldsson and C. Skjoldebrand. Water transport in meat during reheating. *Journal of Food Engineering*, 29:13–21, 1996.

[35] U. Wahlby and C. Skjoldebrand. NIR-measurements of moisture changes in foods. *Journal of Food Engineering*, 47:303–312, 2001.

[36] F. J. Trujillo, C. Wiangkaew, and Q. T. Pham. Drying modeling and water diffusivity in beef meat. *Journal of Food Engineering*, 78:74–85, 2007.

[37] A. Tom, D. Bruneau, K. Alexis, and A. W. Aregba. Desorption isotherms for fresh beef: An experimental and modeling approach. *Meat Science*, 2013.

[38] S. Rahman. Thermal conductivity of four food materials as a single function of porosity and water content. *Journal of Food Engineering*, 15:261–268, 1992.

[39] D-W. Sun and Z. Hu. CFD simulation of coupled heat and mass transfer through porous foods during vacuum cooling process. *International Journal of Refrigeration*, 26:19–27, 2003.

[40] Ch. J. Boukouvalas, M. K. Krokida, Z. B. Maroulis, and D. Marinos-Kouris. Density and porosity: Literature data compilation for foodstuffs. *International Journal of Food Properties*, 9:715–746, 2006.

[41] K. Mc Donald, D-W. Sun, and J. G. Lyng. Effect of vacuum cooling on the thermophysical properties of a cooked beef product. *Journal of Food Engineering*, 52:167–176, 2002.

[42] S. Bakalis, A. Kyritsi, V. T. Karathanos, and S. Yanniotis. Modeling of rice hydration using finite elements. *Journal of Food Engineering*, 94:321 – 325, 2009.